MODELO SIMPLIFICADO Y VALIDACIÓN EXPERIMENTAL PARA COLECTOR CALENTADOR DE AIRE TIPO TUNEL BASADO EN EL FORMALISMO DE COLECTOR PLANO.

Arturo Busso

Departamento de Física, FaCENA , Universidad Nacional del Nordeste - UNNE
Campus Libertad, Av. Libertad 5600, 3400 Corrientes – Argentina; email: ajbusso@exa.unne.edu.ar

ABSTRACT

An adapted formalism valid for flat-plate air solar collectors with single air channel between absorber plate and transparent cover was used to study a tunnel type air solar collector. The model accounts for the particular characteristics of the collector under study, semicircular cross section, geographical location, air as fluid, open circuit, etc., and makes some simplifying assumptions to the real situation.

For the determination of the different heat transfer coefficients, such as internal as external, models found in literature were applied. A model proposed by Mitchell applicable to bodies of complex geometry is used to determine the wind convective coefficient. As for the internal heat transfer coefficient, the collector was considered as rough tube with equivalent diameter dependent on the cross section and perimeter of the real collector.

For the modelling the collector is divided into 10 sections of similar length following the number and position of temperature sensors distributed inside the collector. Energy balance equations are solved for each section being the outcome of one section taken as input for the next section. The resulting system of equations representing the thermal network was solved using the iterative algorithm of Gauss-Seidel and aided by programme written in Visual Basic. Comparison of theoretical and experimental temperature profiles allowed identification characteristic features presented by the profiles.

As conclusion, the adapted formalism allows qualitative analysis of the efficiency curve as well as to determine that for the speeds of air measured in the flow channel, the longitude of the collector is insufficient to reach the maximum temperature attainable at the exit side. Furthermore, characteristic features exhibited by the temperature profiles inside are attributed to deformations in the transparent cover that induce a different rugosity factor for each section.

Keywords: tunnel collector, air solar collector, flat plate collector formalism.

INTRODUCTION

During the years 1993 to 1996 a project on Wood Drying by means of a Natural Convection Solar Dryer (Martina P., Aeberhard A, 1994; Martina P., Aeberhard A, 1995) was carried out jointly by the Departamento de Termodinámica y Máquinas Térmicas de la Facultad de Ingeniería, Universidad Nacional del Nordeste, Chaco, Argentina, and the Institut für Landtechnik Weihenstephan of the Technical University of Munich, Germany.

During this time span a prototype solar wood dryer with 8 m^3 of net capacity was built and put into operation and simulations using the program TRNSYS14.4 (TRNSYS User's Manual, 1994) were done in order to validate the theoretical model describing the drying process for the wood pile (Benkert S., 1995).

As a final stage, the optimization of the drying process was undertaken from the technological point of view in order to get a better understanding of how each of the system's components work and identify construction parameters affecting performance.

This work presents the result of such optimization study made on the tunnel solar air heater.

SIMPLIFIED MODEL

There are numerous works on experimental and theoretical performance of solar air heaters. Most of them deal with flat-plate geometry. This geometry has been worked out extensively by several authors (Duffie J., Beckman W., 1991; Ong K. S. , 1995; Ong K. S. 1996) therefore, the heat balance equations derived from the thermal network describing the system are quite known.

In general terms, the study of the thermal performance involve solving equations resulting from energy balance considerations under steady state conditions. In this way, plate efficiency and heat removal factors are linked to parameters such us air flow rates and heat transfer coefficients (due to surface wind and between moving air streams and the surfaces forming the flow channels).

The derivation of these factors is quite complex and requires considerable effort especially when dealing with design configurations involving geometrical details different from the flat-plate type symmetry.

The theoretical model used for describing the semicircular tunnel collector is an adaptation of the formalism valid for flat-plate collectors, specifically for the single channel design with single airflow between top glass and bottom absorber plate. The model takes into account the particular characteristics of the actual collector; semicircular cross section, 4m in diameter, 60m in length, its location, air as heating fluid, open circuit, etc.

Fig.1. depicts a simplified picture of the heat transfer processes considered to taking place in the tunnel and the associated thermal network.

Because the tunnel collector lies horizontally on the ground, the thermal resistance of the flat plate collector representing back losses to the ambient air is replaced by an equivalent thermal resistance representing the conduction heat losses trough a thin insulation layer to the ground floor.

The following assumptions are made in the model:

- Steady state conditions.
- No absorption of incoming radiation by the transparent plastic cover is considered ($S_1 = 0$ in thermal network).
- One dimensional heat flow in the cover.
- One dimensional heat flow in the ground floor.
- Material properties are independent of temperature.

- The sky is considered as a black body for long wavelengths at an equivalent sky temperature.
- The ground floor temperature is equal to ambient temperature.
- The spectral dependency of transmittance is neglected.
- No effects of dirt or shading on the absorber plate are considered.

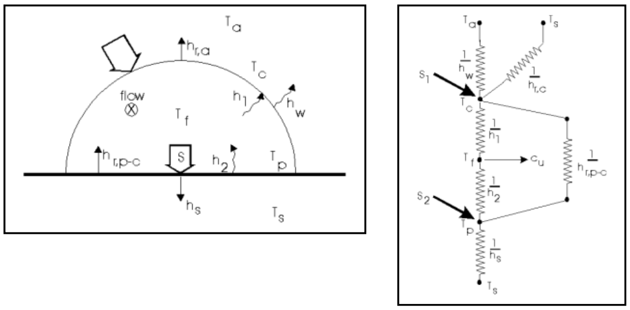

Figure 1.- Simplified model of the heat transfer in the tunnel and associated thermal network.

Part of the energy transferred by the absorbing plate contributes to the heating of the air inside the collector producing the thermal gradient in the direction of the flow. In this way an increasing temperature profile is set up along the collector. The rest of the energy is lost due to various thermal processes, radiation, convection and conduction.

From the thermal network of Fig.1 three heat balance equations can be written for the nodes $\mathbf{T_p}$, $\mathbf{T_c}$ and the point $\mathbf{T_f}$:

$\mathbf{T_c}$: $U_t(T_a - T_c) + h_{r,p-c}(T_p - T_c) + h(T_f - T_c) = 0$ (1)

$\mathbf{T_p}$: $S + h_s(T_a - T_p) + h_{r,p-c}(T_c - T_p) + h(T_f - T_p) = 0$ (2)

$\mathbf{T_f}$: $h(T_c - T_f) + h\ (T_p - T_f) = q_u$ (3)

Where U_t represents the overall top heat transfer coefficient and $U_t = h_w + h_{r,a}$.

Solving eq.(2) for T_p:

$$T_p = \frac{S + h_s T_a + h_{r,p-c} T_c + h_2 T_f}{h_s + h_{r,p-c} + h_2} \qquad (4)$$

replacing (4) in (1):

$$T_c - T_f = \frac{h_{r,p-c} S - (T_f - T_a)(U_t h_s + U_t h_{r,p-c} + U_t h_2 + h_{r,p-c} h_s)}{(U_t + h_{r,p-c} + h_1)(h_s + h_{r,p-c} + h_2) - h_{r,p-c}{}^2} \qquad (5)$$

Similarly, solving eq.(1) for T_c:

$$T_c = \frac{U_t T_a + h_{r,p-c} T_p + h^1 T_f}{U_t + h_{r,p-c} + h_1} \qquad (6)$$

Replacing (6) in (2):

$$T_p - T_f = \frac{S(U_t + h_{r,p-c} + h_1) - (T_f - T_a)(h_s U_t + h_s h_{r,p-c} + h_s h_1 + h_{r,p-c} U_t)}{(U_t + h_{r,p-c} + h_1)(h_s + h_{r,p-c} + h_2) - h_{r,p-c}{}^2} \qquad (7)$$

Substituting eq.(5) and eq.(7) into eq.(3) and working out mathematically one the expression for the useful energy gain per unit length is obtained:

$$q_u = F`[S - U_L(T_f - T_a)] \qquad (8)$$

With collector efficiency factor and the overall heat loss coefficient given by:

$$F` = \frac{h_1 h_{r,p-c} + h_2 U_t + h_2 h_{r,p-c} + h_1 h_2}{(U_t + h_{r,p-c} + h_1)(h_s + h_2 + h_{r,p-c}) - h_{r,p-c}{}^2} \qquad (9)$$

$$U_L = \frac{(h_1 + h_2)[U_t(h_s + h_{r,p-c}) + h_{r,p-c} h_s] + h_1 h_2 (U_t + h_s)}{h_1 h_{r,p-c} + h_2 U_t + h_2 h_{r,p-c} + h_1 h_2} \qquad (10)$$

***Temperature distribution along the flow direction*.**

Eq.(8) represents the energy transferred to the fluid inside the collector. In its path air enters the collector at one end at ambient temperature gaining energy along its way to the other end exiting at a higher temperature, $T_{f,o}$.

In order to study the temperature distribution along the flow direction, lets consider an element of thickness δy in a single air stream at a distance y from the entrance of the collector as shown in Fig.2.

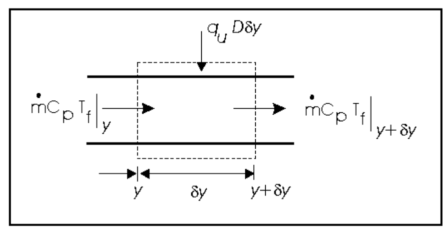

Figure 2.- Heat balance on element along flow direction

In accordance with the assumptions stated previously, the fluid temperature is uniform throughout the cross section of the collector.

The heat balance for this element is:

$$\dot{m} C_p T_f \Big|_y - \dot{m} C_p T_f \Big|_{y+\delta y} + q_u D \delta y = 0 \qquad (11)$$

Replacing (8) in (11), dividing by δy and taking the limit for $\delta y \to 0$ we obtain

$$\dot{m} C_p \frac{dT_f}{dy} - DF`[S - U_L(T_f - T_a)] \qquad (12)$$

Or in a simpler form:

$$\frac{dT_f}{dy} - PT_f = Q \qquad (13)$$

With $P = \frac{DF`U_L}{\dot{m} C_p}$ and $Q = \frac{DF`}{\dot{m} C_p}[S + U_L T_a]$

The general solution for this equation is:

$$T_f = T_a + \frac{S}{U_L} + Ce^{-\frac{DF`U_L}{\dot{m}C_p}y} \tag{14}$$

The value of the constant *C* can be determined applying the BC

$$T_f \Big|_{y=0} = T_a$$

$$T_f = T_a + \frac{S}{U_L} - \frac{S}{U_L} e^{-\frac{DF`U_L}{\dot{m}C_p}y} \tag{15}$$

replacing eq.(15) in eq.(8) the expression for the useful energy gain as a function of the position along the collector is determined:

$$q_u = F'Se^{-\frac{DF'U_L}{\dot{m}C_p}y} \tag{16}$$

Collector efficiency

The instantaneous efficiency is defined as the ratio between the useful energy gain to the solar radiation incident on the device:

$$\eta = \frac{\dot{m}C_p(T_{f,o} - T_{f,i})}{A_c I} \tag{17}$$

Given that $T_{f,i} = T_a$, taking $y = L$ in eq.(15) and replacing in (17) leads to the expression for the efficiency as a function of the mass flow rate:

$$\eta = \frac{\dot{m}C_p S(1 - e^{-\frac{A_c F'U_L}{\dot{m}C_p}})}{A_c I U_L} \tag{18}$$

Fig.3 and Fig.4.- depict a plot of eq.(15), (16) and (18) calculated using values for the different parameters involved valid for a flat plate collector and taken from literature (Duffie J., Beckman W., 1991).

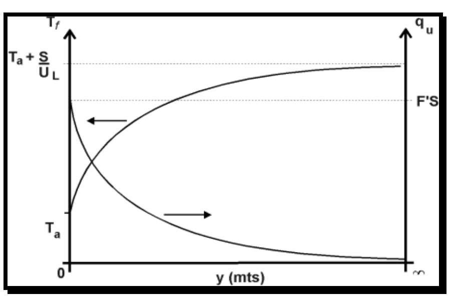

Figure 3.- Useful energy gain and outlet temperature as a function of position along the tunnel collector.

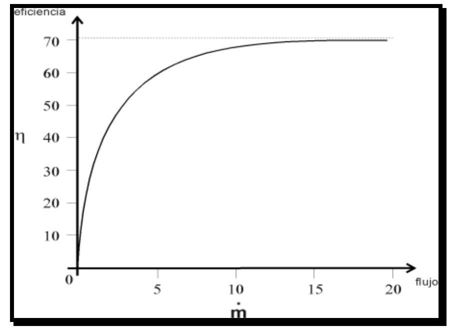

Figure 4.- Efficiency as a function of mass flow rate.

Radiation heat transfer coefficients from cover and absorber surfaces.

The radiation heat transfer between absorber and cover can be found from the expression for the net heat flux between a pair of surfaces (Duffie J., Beckman W., 1991).:

$$Q_1 = -Q_2 = \frac{\sigma(T_2^4 - T_1^4)}{\frac{1-\varepsilon_1}{\varepsilon_1 A_1} + \frac{1}{A_1 F_{12}} + \frac{1-\varepsilon_2}{\varepsilon_2 A_2}} \tag{19}$$

With A_1= absorber area; A_2= cover area; ε_1; ε_1 = surface emittance

The radiation heat transfer coefficient can be obtained by liniarizing eq.(19)

$$Q = Ah_r(T_c - T_p) \tag{20}$$

With

$$h_r = \frac{\sigma(T_2^2 + T_1^2)(T_2 + T_1)}{\frac{1-\varepsilon_1}{\varepsilon_1} + \frac{1}{F_{12}} + \frac{(1-\varepsilon_2)A_1}{\varepsilon_2 A_2}}$$

Assuming $F_{12} = 1$ and due to the geometry of the collector $A_1/A_2 = 2/\pi$ then:

$$h_r = \frac{\sigma(T_c^2 + T_p^2)(T_c + T_p)}{\frac{1-\varepsilon_p}{\varepsilon_p} + 1 + \frac{(1-\varepsilon_2)A_2}{\varepsilon_c \pi}} \tag{21}$$

Sky Radiation

The radiation heat transfer coefficient from the top surface to the sky referred to ambient temperature can be treated as a small object radiating to a large enclosure. In this case, the area ratio $A_1/A_2 \rightarrow 0$ and the view factor F_{12} is unity. Under this conditions eq.(19) becomes:

$$Q = \varepsilon A\sigma(T_{SKY}^4 - T_c^4) \tag{22}$$

With the expression for T_{SKY} given by the relationship proposed by Bliss (1961):

$$T_{SKY} = T_{amb}[0.8 + \frac{T_{dp} - 273}{250}] \tag{23}$$

where T_{pr} represents the dew point temperature.

***Wind induced convection heat transfer coefficient from cover*.**

Due to the complex geometry of the collector the heat transfer coefficient is determined using the model proposed by Mitchell (1976). The model assumes the thermal behavior of the system as being represented by the behavior of a sphere of equal volume and for which the solution is known. Therefore, the expression of the coefficient is given by:

$$h_{wind} = k * \frac{Nus}{R_{eq}} \tag{24}$$

Assuming now the collector be a sphere the Nusselt number is expressed as, $Nus = 0.42 \cdot Re^{0.6}$, where the characteristic length is the cube root of the collector volume.

Internal flux convection heat transfer coefficient

The value for Re > $1x10^5$ inside the collector place the internal flow conditions in the turbulent flow region (Re > 6000).

For the derivation of the internal heat transfer coefficient and to simplify the analysis due to geometry and constructive features, the collector was considered as being a circular rough duct with a diameter equal to the hydraulic or equivalent diameter defined as:

$$D_h = 4\, A_c / P \tag{25}$$

Fig.5 depicts construction details about collector.

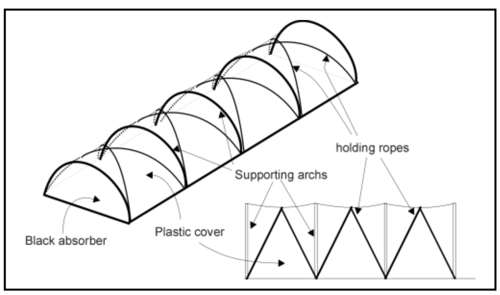

Figure 5.- Constructive details of the tunnel collector

Main sources of internal flow distortion, or roughness, are wrinkles and overhanging of the transparent cover between supporting arches. The latest contribute to an uneven diameter distribution along the length of the collector. In order to account for theses features, a correlation applicable for rough duct and developed by Petukov (1970) which include a friction factor was used for the determination of the Nusselt number:

$$Nu = (Re.\frac{Pr}{X}).(\frac{f}{8})(\frac{\mu}{\mu_w})^n \tag{26}$$

Where for 10^4 < Re > $5x10^6$, $X = 1.07 + 12.7(Pr^{2/3}-1)(f/8)^{1/2}$ and n = 0.11.

SOLUTION PROCEDURE

Because experimental temperature profiles inside the collector were obtained by placing sensors every ten meters apart, the theoretical model assumes the system to be divided into six sections of equal length or short collectors.

It is further assumed that for each section the enclosing walls are at a uniform temperature and that the temperature of the air stream varies linearly along the length of the section.

Physical properties of air inside these sections are assumed to vary linearly with temperature as well.

Under normal circumstances, to solve the set of equations (1), (2) and (3) the values for the various heat transfer coefficients involved are needed. This in turn, implies *a priori* knowledge of $\mathbf{T_c}$, $\mathbf{T_f}$ and $\mathbf{T_p}$, which is not the case.

Therefore, the solution procedure begins giving an initial guessed set of values to enclosing wall and mean air temperature of the first section and from them the corresponding heat transfer coefficients evaluated. With these heat transfer coefficients a new set of temperatures is determined solving the set of eq. (1), (2) and (3) and comparing them with the previously assumed ones. The iterative process is repeated until convergence is reached, this is, all consecutive mean temperatures differ by less than 0.01 ºC.

Upon convergence the next section is treated following the same iterative procedure described before. Here, initial wall and air temperatures are set to the mean values of corresponding variables in the previous section. Moreover, air inlet temperature is equal to air outlet temperature of the previous section.

The iterative process is than repeated until all the sections of the given collector are considered.

A computer program was written in Visual Basic 4 to solve the system of equations (1), (2), (3) using a Gauss-Seidel iterative algorithm. It's been observed that convergence is reached within the fourth iteration. The program follows the same computation logic as described above and predicts $\mathbf{T_c}$, $\mathbf{T_f}$ and $\mathbf{T_p}$ for each section.

Fig.6. shows the flowchart for the computer program generated.

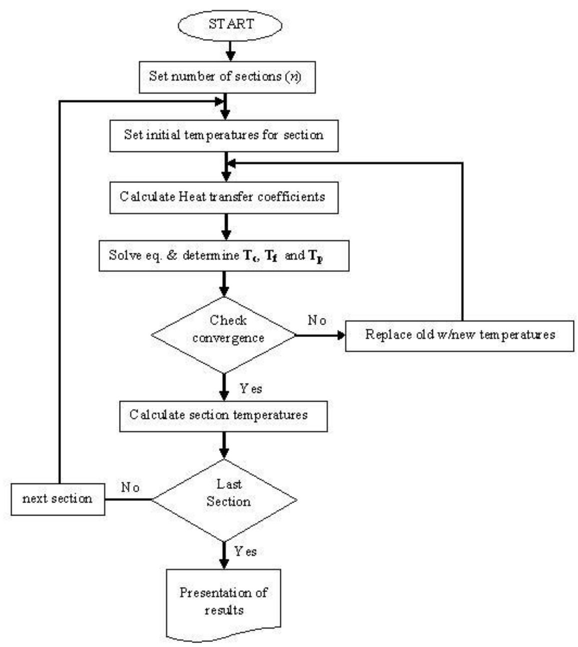

Figure 6.- Flowchart of computer program generated application.

Results from the calculation are presented graphically plotting predicted and experimental temperature profile and allows sensitivity analysis by parameter variation and recalculation. In this manner solar radiation, wind speed, absorption and emittance coefficient, among others can be varied.

In addition, the program also includes two modes of calculation, constant same-for-all-sections or variable constant-by-section friction coefficient.

RESULTS

Values for the absorbance, transmittance and emittance of the black absorber and transparent cover were taken from tables. It was observed that variations in the values of these parameters or in the wind speed produced only a difference of the order of ± 1ºC in the calculated air output temperature indicating that the theoretical model does not depend strongly on them.

On the contrary, large differences were obtained when either the thermal conductivity coefficient or thickness of the bottom insulating material were varied.

Fig.7. is a plot of experimental and predicted by eq. (15) and (16)] air output temperature and efficiency as a function of mass rate. Predicted values were calculated on the basis of heat transfer coefficients taken from literature for a flat plate collector therefore the difference between the curves. Nevertheless, a good functional correlation is observed.

Fig.8. presents typical air temperature profiles as a function position inside the collector for different years and different intensity of incident solar radiation. The entrance of the collector is taken as origin of coordinate.

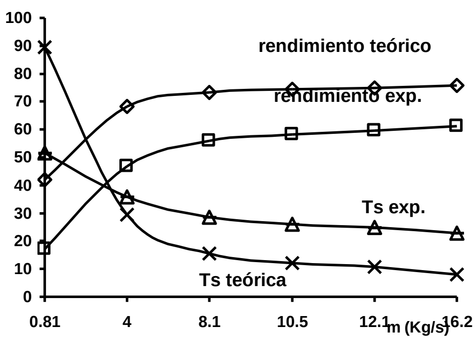

Figure 7. Output air temperature $\mathbf{T_s}$ and η as function $\dot{m}$

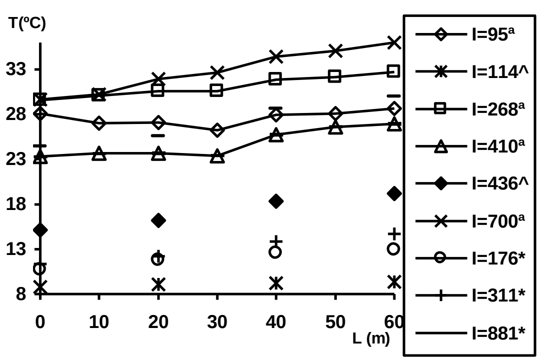

Figure 8.- Temperature profiles for years ^ ´94, * ´95, ª ´97 and different solar radiation

In general, the curves are not smooth and a decrease of air temperature is evident midway in the collector (L = 30 m). This feature persisted even using different sensor at the same position indicating it was not measurement related.

The depression is possibly attributed to variations of the internal flux convection heat transfer coefficient due to a variable friction factor along the length of the collector.

To test this hypothesis, simulations were performed allowing for the friction factor to take different values in each section. Fig.9. shows the outcome of such a simulation. An improvement in the correlation is noticeable. Temperature difference between experimental and simulated air output temperature was reduced from a value of 1.5 ºC before correction to 0.5 ºC after applying the correction.

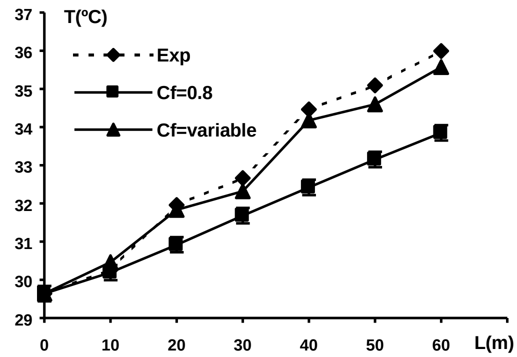

Figure 9.- Comparison of experimental and simulated air output temperatures for constant and variable friction factor.

CONCLUSIONS

An adapted theoretical model to predict the response of a tunnel type air solar collector was presented. The inherent mathematical complications due to the geometry of the system were simplified adapting the formalism valid for flat plate air solar collectors taking into account the peculiar characteristics of our collector.

The model allowed a qualitative analysis of the efficiency curves and to relate constructive characteristics with operation performance so as to determine that for air speeds measured in the flow channel, the longitude of the collector is insufficient to reach the maximum temperature attainable at the exit side.

Furthermore, characteristic features exhibited by the temperature profiles inside are attributed to deformations in the transparent cover that induce a different rugosity factor for each section. Correction of the model to account for this assumption allowed the precision in the be in ± 0.5 ºC in some cases.

REFERENCES

Bliss R.W., (1961). Atmospheric Radiaction Near the Surface of the Ground. Solar Energy, 5, 103,

Benkert S., (1995). Modellierung und Experimentelle Uberprufung einer Pilotanlage zur solaren Holztrocknung, Universidad Técnica de Munich.

Duffie J., Beckman W., (1991). Solar Engineering of Thermal Processes, 2da. edición, Wiley, New York.

Martina P., Aeberhard A., (1994). Secado Solar de Maderas Mediante Secadero Solar de Convección Natural. Scholarship Report. Dpto. de Termodinámica, Fac. de Ingeniería, UNNE.

Martina P., Aeberhard A., (1995). Optimización de Secado Solar de Maderas Mediante Secadero Solar de Convección Natural. Scholarship report. Dpto. de Termodinámica, Fac. de Ing., UNNE.

Manual del Usuario del TRNSYS 14.1, Universidad de Wisconsin, Madison, 1994.

Mitchell J.W., (1976). Heat Transfer from Spheres and other Animal Forms. Biophysical Journal, 16, 561.

Ong K. S., Thermal Performance of Solar Air Heaters, Solar Energy, 55, 93-109 (1995).

Ong K. S., Thermal Performance of Solar Air Heaters - Experimental Correlation, Solar Energy, 55, 209-220 (1995).

Petukhov B. S., Heat Transfer and Friction in Turbulent Pipe Flow with Variable Physical Properties, In Advances in Heat Transfer, J. P. Hartnett and T. F. Uirvine (Eds). pp. 504-564. Academic Press, New York (1970).